INDO AMERICAN JOURNAL OF PHARMACEUTICAL RESEARCH

INSILICO DOCKING AND MOLECULAR DYNAMIC SIMULATION STUDIES OF NUCLEOCAPSID PROTEIN FROM HUMAN T-LYMPHOTROPHIC VIRUS

Ummehani A. Kallawala, Sharav A. Desai*, Dhananjay B. Meshram

Department of In-Silico Drug Discovery & Design, Pioneer Pharmacy Degree College, Vadodara-390019, Gujarat, India.

ARTICLE INFO

Article history
Received 31/12/2021
Available online
31/01/2021

Keywords
HTLV-1,
Molecular Docking,
Simulation,
Nucleocapsid,
RMSD,
RMSF.

ABSTRACT

This work was conducted to find out a natural compound capable of inhibiting the Nucleocapsid protein present in the HTLV-1 virus. HTLV-1 virus belongs to delta retroviruses that do not contain protooncogene in their genome. Computer-aided drug design approach was used to obtain inhibitory compounds. A total of 109 natural compounds were identified by conducting a literature survey. PubChem database was utilized to retrieve the compound structure in 2D format. HTLV-1 NC (Nucleocapsid) protein was taken from the protein data bank. Molecular docking method was used to find out the compound capable of binding with the target protein. Compounds with good binding affinity were selected and further ADMET analysis was done. The final list of the compound with satisfactory ADMET profile and binding score were scrutinized using protein and ligand interaction results. The compound Miraxanthine_V was found to have a good binding affinity with said ADMET properties and was further studied for its structural stability with the target protein. Molecular dynamic simulation studies for 10 ns were done to check the stability of the protein and ligand complex during a simulation. Parameters like RMSD, RMSF, and radius of gyration were observed to understand the fluctuations and stability. the values obtained with simulations were found to come under the acceptance limit. We are proposing Miraxanthine_V as a potential inhibitor for HTLV- infection.

Corresponding author
Dr. Sharav A. Desai
Associate Professor,
Department of InSilico Drug Discovery & Design
Pioneer Pharmacy Degree College,
Vadodara-39009-Gujarat, India.
+91-9428128137
sharavdesai@gmail.com

*Please cite this article in press as **Dr. Sharav A. Desai** et al. Insilico Docking and Molecular Dynamic Simulation Studies of Nucleocapsid Protein from Human T-Lymphotrophic Virus. Indo American Journal of Pharmaceutical Research.2021:11(01).*

INTRODUCTION

Human T-Cell Lymphotropic virus type (HTLV-I) is an oncogenic retrovirus that exhibits specific tropism for human T-cells. Approximately 1 to 4 % of HTLV-I infected individual develops Adult T-Cell leukemia (ADL) or HTLV-I associated myelopathy, a slowly progressive neurologic disorder[1]. Human T- Lymphotropic viruses HTLV, comprises a four related retroviruses family that affect T- Cells. The viruses were found to have an origin of transmission through monkeys in to humans. The discovery of the first retrovirus proceeded in japan and the united states independently and identified as human T-cell leukemia virus in the T-Cell line from a patient with cutaneous T-cell lymphoma[2-3]. After the discovery of HTLV-1, another retrovirus was described and was named HTLV-2. HTLV-2 was found to have a similar genome structure and shares around 70% of nucleotide sequence homology with HTLV-1. In 2005 two more HTLV-2 and HTLV-4 were reported from central Africa. At present HTLV-1 is convincingly found as the culprit for human diseases[4-5]. The most important route of transmission was found to be from mother to child through breastfeeding. Other routes of transmission include sexual intercourse and blood contact including transfusion of infected cellular products and exchange of syringes and needles[6–8]. After transmission the reverse transcriptase generates proviral DNA from RNA and the through virus integrase, the provirus inserts itself into the host genome. Infection is thought to spread by dividing cells with very little particle production[9]. As the number of cells with provirus increases the severity of the infection is also increases. Viral *tax* gene expression is known to cause the increase in proliferation of infected cells and also known to reduce the rate of apoptosis of infected cells[10]. HTLV-I infections are known to cause subclinical immune suppression and it can become an outcome for opportunistic coinfections like tuberculosis and strongyloidiasis. Conditions like arthritis, UTIs, fibromyalgia, depressions are also found in major populations infected with HTLV-I infections[11–14].

We have selected HTLV_Nucleocapsid protein as our target for molecular docking and dynamic analysis. HTLV-1 and HIV share many common structural and functional proteins with each other. Our target protein Nucleocapsid is also a common protein between HTLV-1 and other retroviruses including HIV. The HTLV-1 NC protein like HIV-1 NC contains two zinc finger motifs, but the overall amino acid sequence of the HIV-1 is basic, whereas the HTLV-1 NC is a nucleocapsid protein. Like all retrovirus, HTLV-1 also undergoes minus-strand transfer in which part of minus-strand stop DNA must anneal to the viral RNA. This process of strand transfer involves both the destabilization and annealing events. It is being now well understood that the Nucleocapsid protein of retrovirus functions by accoupling themselves in annealing of viral TAR RNA to the complementary sequence in minus-strand strong stop DNA[15]. Targeting the Nucleocapsid protein will surely disturb the reverse transcription of retrovirus and the agents inhibiting the actions can come out as potential therapeutic candidates for HTLV-1 infections.

As, it is very much clear that if we follow the traditional drug discovery approach to find a suitable drug for HTLV-1, it may take several years and we cannot afford to lose many of our lives during such a long process. Today we have high computation power with all the necessary information available online and most of them are free. We can fasten the discovery process by using molecular docking and molecular dynamic simulation studies to narrow down our selection for the antiviral compounds at the very initial stage of our process. Even we don't need to have those compounds physically to test their effectiveness and also, we don't need to handle such an infectious virus. It is being always observed that natural compounds so far have been found to have many of the therapeutic antiviral effects. We have searched the literature and found 109 natural compounds, which can come out as a potential therapeutic candidate for HTLV-1 infection. We have used binding affinity and simulation parameters to scrutinizes our selected 109 natural ligands.

MATERIAL AND METHOD

Protein structure preparation

The X-ray diffraction-based crystal structure of HTLV -I Capsid protein (PDB ID:1QRJ) with a resolution of 1.80 Å was taken from the protein data bank. The structure was cleaned to ensure maximum quality and reliability. The bound ligands, water molecules were removed and missing atoms and residues were added. Steric clashes were minimized and hydrogen atoms were added. Formal bond orders were determined, side chains were optimized and fixed, charges added using program implemented in chimera, SWISS PDB viewer, and Chiron minimization and refinement tools[16–19].

Computational screening

It is being observed that natural compounds do have antimicrobial properties and currently we also have a large number of compounds coming from natural sources. So, we have directed our findings towards the natural compounds, which can come out as potential therapeutic candidates for HTLV-I infections. After an extensive literature survey, we found a total of 109 compounds that we can use to bind with our target HTLV-Capsid protein. The found compounds were retrieved from the PubChem database in the 2D structure. The compounds were imported in to the PyRx (V 8.0)[20] and energy minimization was done using the Open Babel (Version 2.3.1) module of the same software[21]. Energy minimization was done via the Universal force field (UFF) using the conjugate gradient algorithm. A total number of 200 steps were set and the number of steps to update was set to 1. The minimization was set to stop at an energy difference of less than 0.1 Kcal/mol[22-23].

Docking studies

Molecular docking was performed with PyRx (V 8.0), which is an extension of the python molecular viewer. A Lamarckian genetic algorithm was used to perform the automated molecular docking of the protein with each ligand[24-25]. The torsion bonds and side chains were kept to rotate freely, while the protein structure was kept rigid[26]. Gasteiger charges were computed, and all the charges of non-polar hydrogens were assigned. The grid map was set at 60×60×60× and the grid was spaced at 0.375Å. Both selected ligand and protein were converted in to pdbqt structure format. Protein and ligands were loaded in to PyRx as macromolecule and ligand, respectively. All the compounds were docked and affinity was calculated in kilocalories per mole[26].

ADME and Toxicity predictions

The selected compounds with good binding energies were further studied for their Adsorption, distribution, excretion, metabolism, and toxicity profile using SWISS ADME and data warrior tools. The predicted properties considered were blood-brain barrier penetration properties, Human intestinal absorption, inhibition to cytochrome P450 enzyme, and bioavailability. Compounds showing satisfactory properties were further studied for their toxicity profile using data warrior tools. Toxicity profiles included were mutagenicity, tumorigenicity, irritability, reproducibility, Ames toxicity, and carcinogens[27-28].

Molecular Dynamic Simulation

Docked protein and ligand complexes were subjected to molecular dynamics simulation using NAMD software[29-30]. The success of MD simulation depends on the selection of the initial protein and ligand structures. Initially, the structure was checked for inconsistencies. Out of 53 selected compounds from the docking results, based on the ADME analysis and other molecular properties, we have selected the final Miraxanthine_V compounds having a PubChem number 135438594. The docked complexes were studied for their stability during the simulation. The root means square deviation, root mean square fluctuation, and radius of gyration was studied for protein backbone and ligand within the binding site of the simulated system[31-32]. The stabilities of the complexes were examined by monitoring their root mean square deviation (RMSD) during 50,00,000 steps for a 10 ns simulation. MD simulations were performed using the CHARMM36 force field. Visual molecular dynamics (VMD) was used to generate PSF files for all complexes[33]. Protein and ligand complex were solvated in cubic water boxes containing transferable intermolecular potential with 3 points (TIP3P) water molecules. The box size was chosen to match the molecular dimensions so that there was a distance of 5˚A between the protein surface and the edges of the periodic box. A 5˚A cut off distance was used to calculate short-range nonbonded interactions. The particle mesh Ewald (PME) method was used to calculate long-range electrostatic interactions[34]. The SHAKE method was used to constrain all bonds involving hydrogen atoms. A conjugated gradient system was used for energy minimization, with all parameters set to default[35-36]. The system first performed 10000 steps of Conjugated gradient with energy minimization. We used Langevin Dynamics with pressure control so our system was not an NVT ensemble[37]. The Nose–Hoover method was used to maintain a constant temperature[38]. The time step of each simulation was set to 2 fs. Visualizations and data analysis were performed with VMD software.

RESULT AND DISCUSSION

Virtual Screening

Virtual screening helps us to screen the biological molecules with good binding affinity. In this study, we have used PyRx 8.0 tool to screen out the molecules. A total of 105 natural ligands were selected and were docked to the target protein. The docked compounds were examined in the Auto dock tool and binding free energy was calculated[39]. We have selected a total of 53 compounds on their binding affinity ranging from -7.5 to -6.0 kcal/mol.

Table 1. Molecular Properties of the Selected Compounds.

PubChem Compound IDs	H-Bond Acceptor	H-Bond Donor	Molecular Weight	Total Polar Surface Area	cLogP	cLogS	Drug likeness
5281176	6	3	211.17	104	-3.6534	-0.807	-3.3451
11953905	23	11	902.8	381	-8.14	-3.114	-2.6419
5281121	22	11	867.8	347	-3.7901	-2.617	-11.87
11953907	24	12	870.7	409	-10.052	-1.847	-1.1528
11953899	18	9	735.7	288	-2.555	-2.788	-11.39
6325294	17	8	726.6	285	-5.9533	-3.432	-0.41194
11953903	19	11	712.6	329	-9.6323	-1.46	-4.0374
6325284	20	11	726.6	346	-9.9819	-1.442	-0.85264
72193633	7	7	580.7	226	1.2127	-5.029	0.15349
45485025	6	7	550.7	217	1.2827	-5.011	0.070246
6325833	17	8	630.5	301	-8.5816	-0.614	-4.3902
11953901	14	8	550.5	249	-7.7952	-1.76	-2.8974
6325438	14	8	550.5	249	-7.7952	-1.76	-2.8974
6096868	14	8	550.5	249	-7.7952	-1.76	-2.8974
656521	13	8	473.4	223	-3.5775	-1.009	-10.071
656516	12	7	457.4	202	-3.0796	-1.119	-10.019
71448975	3	2	319.4	58.6	4.2583	-3.588	-10.865
656493	11	6	427.4	182	-2.4776	-1.248	-10.383
184959	11	6	427.4	182	-2.4776	-1.248	-10.383
1548943	3	2	305.4	58.6	3.8039	-3.318	-10.379
135871118	8	4	360.4	128	-2.3184	-2.02	1.7398
135438589	10	6	390.3	177	-3.5111	-1.559	0.85333
135438597	9	5	374.3	157	-3.1654	-1.855	0.85333
6324770	9	5	388.3	170	-5.8059	-1.874	0.6039
135438596	12	5	420.3	200	-5.1725	-1.396	-2.2646
11953911	11	4	418.3	193	-7.7285	-1.08	-0.22642
656565	12	5	478.5	214	-0.4114	-2.785	1.2532
135438594	8	5	346.3	139	-2.5941	-1.706	1.671
135438593	7	4	330.33	119	-2.2484	-2.002	1.671
46173992	7	5	345.33	130	-2.7783	-2.021	0.215
119301	12	7	409.39	202	-3.6382	-0.512	-13.537
656506	11	6	448.5	216	-0.7099	-0.648	1.1862
441537	14	6	528.5	268	-3.4116	-2.25	1.6089
656555	11	5	423.5	200	-0.2949	-0.393	-1.3547
5281207	8	4	348.31	173	-10.807	-0.504	-3.6595
49787014	10	5	360.32	173	-3.4122	0.052	-7.5295
656498	11	5	409.4	200	-0.7493	-0.123	-0.42771
656568	12	6	425.4	220	-1.095	0.173	0.025231
135438591	10	4	358.37	173	-5.5711	-0.578	-0.28187
135438590	9	5	326.3	157	-4.2795	-1.049	-4.7185
441473	8	5	311.29	143	-1.5882	-1.123	-10.071
161355	8	5	311.29	143	-1.5882	-1.123	-10.071
107721	8	5	311.29	143	-1.5882	-1.123	-10.071
119033	7	4	295.29	123	-1.2425	-1.419	-10.071
5281124	11	6	359.28	198	-1.9596	-0.731	-7.9479
135438599	9	5	339.3	179	-5.0269	-1.107	0.39745
135438600	10	5	340.28	174	-4.6291	-1.031	-0.20828
6325831	8	4	324.29	150	-7.2083	-0.403	0.96924
6096870	7	3	308.29	130	-6.3562	-0.802	-0.4461
135438595	10	5	351.27	175	-5.6707	-1.366	-0.31811

135438592	10	5	326.26	174	-5.0835	-0.761	1.3293
135438598	8	4	268.22	136	-4.6209	-0.638	0.1494

ADMET analysis

We have selected 53 compounds and the same compounds were studied for their ADMET properties. The properties like Human intestinal absorption, irritability, reproductive effect, inhibition to cytochrome p450 enzyme, and several others were predicted. It is clear from the results that compound number 135438594,135438593, 135871118, 71448975, 5281176, 1548943, 119033, and 46173992 have a high intestinal absorption value (**Error! Reference source not found.**).

Table 2. ADMET analysis with the Lowest Binding affinity.

Molecule	GI absorption	BBB permeant	Pgp substrate	CYP2D6 inhibitor	Mutagenic	Tumorigenic	Reproductive Effective	Irritant	Binding Affinity
135871118	High	No	Yes	No	none	none	none	none	-7.2
135438600	Low	No	No	No	none	none	none	none	-6.5
135438599	Low	No	No	No	none	none	none	none	-6.5
135438598	Low	No	No	No	none	none	none	none	-6.2
135438597	Low	No	No	No	none	none	none	none	-7.2
135438596	Low	No	No	No	none	none	none	none	-7.5
135438595	Low	No	No	No	none	none	none	none	-7.4
135438594	High	No	No	No	none	none	none	none	-7.5
135438593	High	No	No	No	none	none	none	none	-7.1
135438592	Low	No	No	No	none	none	none	none	-6.6
135438591	Low	No	No	No	none	none	none	none	-6.4
135438590	Low	No	No	No	none	none	none	none	-6.5
135438589	Low	No	No	No	none	none	none	none	-6.9
72193633	Low	No	Yes	No	none	none	none	none	-7
71448975	High	Yes	No	Yes	none	none	none	high	-6
49787014	Low	No	No	No	high	none	high	high	-6.4
46173992	High	No	No	No	none	none	none	none	-6.9
45485025	Low	No	Yes	No	none	none	none	none	-7.4
11953911	Low	No	No	No	none	none	none	none	-7.6
11953907	Low	No	Yes	No	none	none	none	none	-6.7
11953905	Low	No	Yes	No	none	none	none	none	-6.4
11953903	Low	No	No	No	none	none	none	none	-7
11953901	Low	No	No	No	none	none	none	none	-7.6
11953899	Low	No	No	No	high	none	high	high	-7.4
6325833	Low	No	No	No	none	none	none	none	-7.6
6325831	Low	No	No	No	none	none	none	none	-6.2
6325438	Low	No	No	No	none	none	none	none	-7.9
6325294	Low	No	Yes	No	none	none	none	none	-6.6
6325284	Low	No	Yes	No	none	none	none	none	-7.3
6324770	Low	No	No	No	none	none	none	none	-7.5
6096870	Low	No	No	No	none	none	none	none	-6.8
6096868	Low	No	No	No	none	none	none	none	-7.7
5281207	Low	No	No	No	none	none	none	none	-7.1
5281176	High	No	No	No	low	high	none	low	-6
5281124	Low	No	No	No	high	none	high	high	-6.2
5281121	Low	No	Yes	No	high	none	high	high	-7
1548943	High	Yes	No	Yes	none	none	none	none	-6
656568	Low	No	No	No	none	none	high	none	-6.1
656565	Low	No	Yes	No	high	low	high	none	-6.9
656555	Low	No	Yes	No	none	none	high	none	-6.5
656521	Low	No	No	No	high	none	high	high	-6.4
656516	Low	No	No	No	high	none	high	high	-6.9
656506	Low	No	No	No	none	none	high	none	-6.7
656498	Low	No	Yes	No	none	none	high	none	-6.4
656493	Low	No	No	No	high	none	high	high	-6.9
441537	Low	No	Yes	No	none	none	high	none	-6.6
441473	Low	No	No	No	high	none	high	high	-6.6

184959	Low	No	No	No	high	none	high	high	-6.9
161355	Low	No	No	No	high	none	high	high	-6.5
119301	Low	No	Yes	No	high	low	high	high	-6.3
119033	High	No	No	No	high	none	high	high	-6.2
107721	Low	No	No	No	high	none	high	high	-6.5

From **Error! Reference source not found.**, it is also observed that we have compounds with high intestinal absorption values but at the same time several of them are also showing their inhibitory properties towards the Cytochrome P450 enzymes, so such compounds were removed from the further selections. Similarly, the selected compounds with high intestinal absorption values and negative inhibitory actions to cytochrome P450 enzymes were also studied for their mutagenic, tumorigenic, irritability, and reproductive effect and their ability to bind pGp substrate protein. Table no 2 indicates that compounds number 135871118, 71448975, 5281176, and 1548943 have either of the said effects, so these compounds were also removed from the study. Finally, we selected three ligands namely Miraxanthine_V_135438594, Miraxanthine_V _CID_135438593, and 2-Descarboxy-Betanidin _CID_46173992 for further analysis. Among these three ligands obtained, we have selected Miraxanthine_V for further investigation. Miraxanthine_V has shown the highest binding affinity towards the target protein compares to the other two.

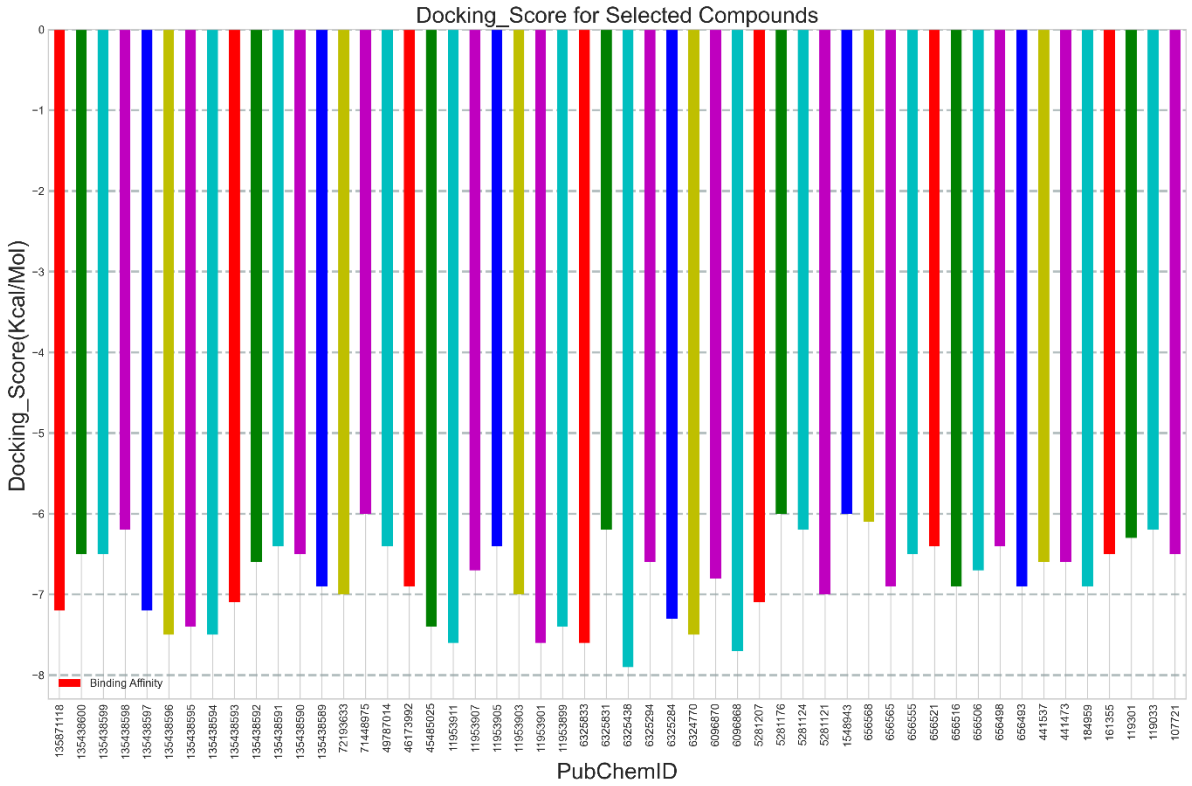

Figure 1. Selected Compounds & Binding affinity.

Protein-ligand interaction

The hydrogen bond and hydrophobic interactions of the protein-ligand complex was analyzed by LigPlot+ (v 1.4.5)38 and Protein-ligand interaction profiler. "LigPlot+" is a graphical system that generates multiple two-dimensional (2D) diagrams of ligand-protein interactions from docked complexes. PLIP is complementary to another state-of-the-art tool like a swiss dock, galaxy site, or ProBis and thus it was also used to study the protein-ligand complex. The server allows comprehensive detection and visualization of protein and ligand complexes along with interaction patterns[40-41].

Table 3. Hydrophobic Interaction between protein and ligand.

Index	Residue	AA	Distance	Ligand Atom	Protein Atom
1	37A	PHE	3.52	3348	551

Table 4. Hydrogen bond interaction between protein and ligand.

Index	Residue	AA	Distance H-A	Distance D-A	Donor Angle	Protein donor?	Sidechain	Donor Atom	Acceptor Atom
1	30A	ALA	3.12	3.95	147.13	No	No	3345 [O.co2]	473 [O2]
2	33A	GLY	2.83	3.35	112.65	Yes	No	498 [Nam]	3355 [O2]
3	34A	SER	2.55	3.13	116.71	Yes	No	505 [Nam]	3355 [O2]
4	60A	GLN	2.31	3.07	134.52	No	No	3374 [O3]	943 [O2]
5	63A	CYS	2.53	3.09	116.58	No	No	3372 [O3]	994 [O2]
6	126A	GLY	1.85	2.70	137.80	No	No	3351 [Npl]	1959 [O2]

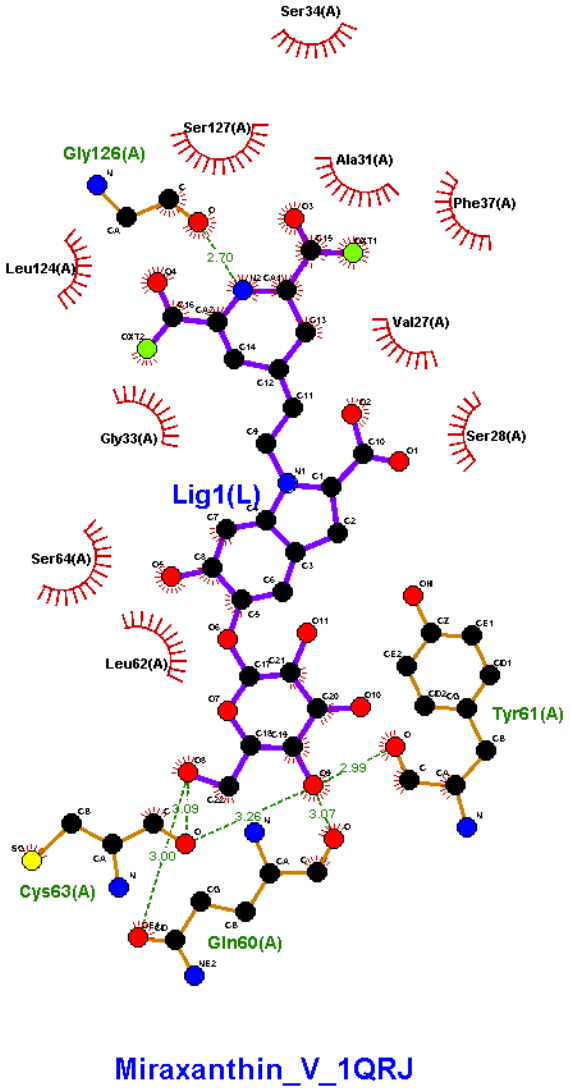

Figure 2 Protein and Ligand interaction Diagram.

Molecular Dynamic Simulation studies

We assessed the residue RMSD, to study the residue behavior of the protein during the simulations. In general, a residue's RMSD value was considered to represent the local flexibility of a protein and Mirxanthin_V complex. It reflected the mobility of an atom during the MD simulation trajectory. Therefore, a higher residue RMSD value indicated higher mobility; conversely, a lower residue RMSD value indicates lower mobility. To investigate the fluctuations in the ligand-binding energy as well as the motions of the amino acid residues within the complex during the simulation, the root means square fluctuation (RMSF) of the complex was also monitored. Besides, root means square gyration was also calculated to monitor the compactness of the complex and how the structure folded, unfolded during simulation[42].

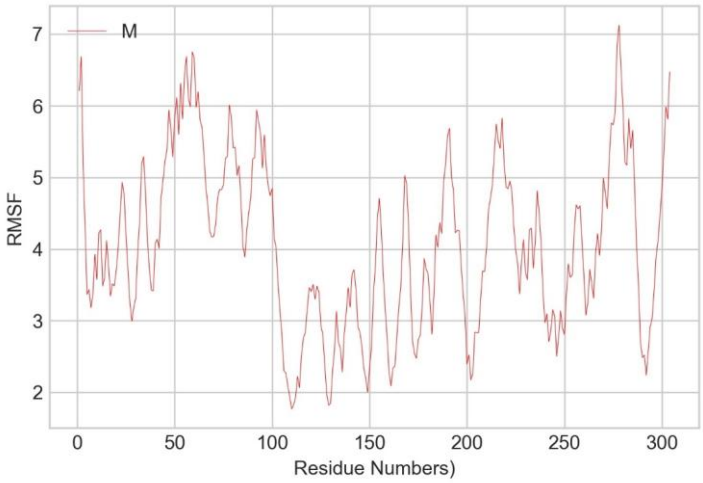

Figure 3. RMSF results for Miraxanthine_V with 1QRJ protein, based on the data from 10 ns simulation.

The root means square fluctuations (RMSF) were assessed and plotted to equate the flexibility of each residue in the–ligand-protein complexes. The RMSF of the protein-ligand complex denoted the minimized fluctuation for all the complexes. The RMSF did not deviate much during the simulation period of 10 ns and the average RMSF values were kept constant for all the complexes.

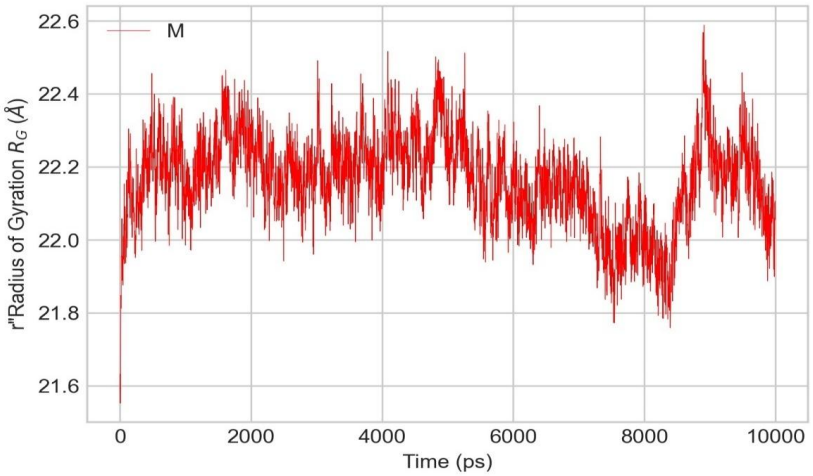

Figure 4. The radius of Gyration results for Miraxanthine_V with 1QRJ protein, based on the data from the 10 ns simulation.

The radius of gyration was also monitored during the 10-ns MD simulation for each protein-ligand complex to ascertain whether the complex was stably folded or unfolded. If the radius of gyration remained relatively constant, the complex was considered to be stably folded, otherwise, it was considered to be unfolded.

In this study, the radius of gyration values obtained is shown in figure 3. All the values obtained for the test ligand Miraxanthine_V showed a relatively constant radius gyration during the simulation and are close to the mean radius of gyration values of protein and ligand complex. So, we can conclude that the complex formed relatively stable folded polypeptide structures during the 10-ns MD simulation.

Table 5. RMSD values for the simulated complexes.

Protein-Ligand complex	Mean RMSD (Å)	Min RMSD (Å)	Max RMSD (Å)
1QRJ-Miraxanthin_V	1.881	0.86	2.71

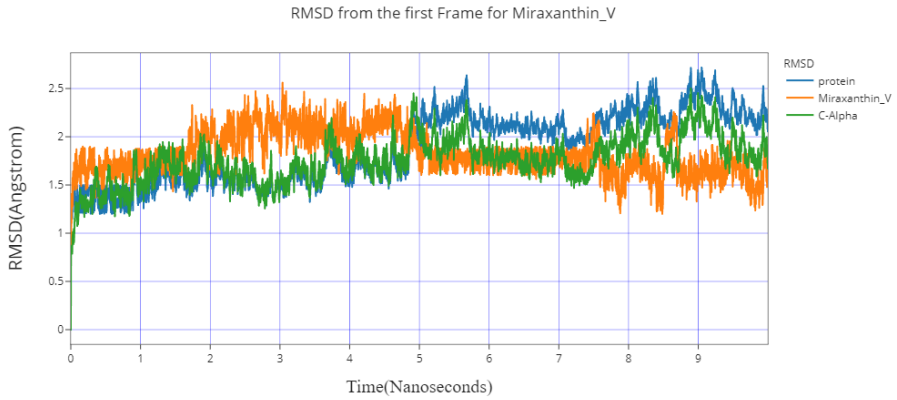

Figure 5. RMSD results for Miraxanthine_V with 1QRJ protein, based on 10 ns simulation.

The RMSD values presented in the table for protein and ligand complex were obtained during their 10 ns simulation. It is clear from the RMSD values that complex found stable during the simulation with values between 1 to 3 (Å). It is also observed from the graphs that the complex was also equilibrated as the average RMSD values are stabilized at the end of the 10 ns simulation. This fixed range of RMSD was indicating the interaction between bound ligand and flexible loop region, as it reduces the flexibility of the protein-ligand complex.

CONCLUSION

As our current understating of viral disorder makes us clear that we have to keep developing new inhibitor compounds. In the same sense, we have tried to find out natural compounds which can come out as potential therapeutic inhibitor for HTLV- 1 infection. Instead of going for the traditional drug discovery approach, we have used Computer-aided drug design to achieve our goal. An extensive literature survey was conducted and we found 109 compounds with some antiviral properties. Molecular docking, ADME profile, and Molecular dynamic simulation studies ended with one compound Miraxanthine_V, which we are proposing as an active ligand.

Recommendations:

We are recommending In-vitro antiviral assay and further conformational studies to be conducted on Miraxanthine_V and its actions against HTLV-1 infections.

Funding: The study was funded by the author.

COMPETING INTERESTS:

The authors declare that they have no conflict of interest

ACKNOWLEDGEMENTS

All the authors are thankful to Shri. D.D. Patel, President Pioneer Medical and Paramedical Institutes for providing necessary computational facility to carry out the research work.

Abbreviations:

ADME : Absorption, Distribution, Metabolism, Excretion
HTLV : Human T-Lymphotropic virus
RMSD : Root Mean Square Deviation
RMSF : Root Mean Square Fluctuation
RGYR : Radius of Gyration
Ps : Picoseconds
Ns : Nanoseconds
MD : Molecular Dynamics
AA : Amino acid
GI : Gastro intestinal
BBB : Blood brain barrier
CYP : Cytochrome Protein
UFF : Universal Force Field
PDB : Protein Data Bank

REFERENCES

1. Khorasanizadeh S, Campos-Olivas R, Summers MF. Solution structure of the capsid protein from the human T-cell leukemia virus type-1. J Mol Biol. 1999 Aug;291(2):491–505.
2. Poiesz BJ, Ruscetti FW, Gazdar AF, Bunn PA, Minna JD, Gallo RC. Detection and isolation of type C retrovirus particles from fresh and cultured lymphocytes of a patient with cutaneous T-cell lymphoma. Proc Natl Acad Sci U S A [Internet]. 1980 Dec;77(12 II):7415–9. Available from: https://pubmed.ncbi.nlm.nih.gov/6261256
3. Gallo RC. History of the discoveries of the first human retroviruses: HTLV-1 and HTLV-2. Oncogene. 2005 Sep;24(39):5926–30.
4. Blattner WA. The epidemiology of the human T-cell lymphotrophic virus type I and type II: etiologic role in human disease. Transfusion. 1991 Jan;31(1):67–75.
5. Mahieux R, Gessain A. The human HTLV-3 and HTLV-4 retroviruses: New members of the HTLV family. Pathol Biol. 2009 Mar;57(2):161–6.
6. Biggar RJ, Ng J, Kim N, Hisada M, Li HC, Cranston B, et al. Human leukocyte antigen concordance and the transmission risk via breast-feeding of human T cell lymphotropic virus type I. J Infect Dis. 2006 Jan;193(2):277–82.
7. Fujino T, Nagata Y. HTLV-I transmission from mother to child. J Reprod Immunol. 2000 Jul;47(2):197–206.
8. Proietti FA, Carneiro-Proietti ABF, Catalan-Soares BC, Murphy EL. Global epidemiology of HTLV-I infection and associated diseases. Oncogene. 2005 Sep;24(39):6058–68.
9. Gonçalves DU, Proietti FA, Ribas JGR, Araújo MG, Pinheiro SR, Guedes AC, et al. Epidemiology, treatment, and prevention of human T-cell leukemia virus type 1-associated diseases. Clin Microbiol Rev. 2010 Jul;23(3):577–89.
10. Taylor GP, Matsuoka M. Natural history of adult T-cell leukemia/lymphoma and approaches to therapy. Oncogene. 2005 Sep;24(39):6047–57.
11. Cruz BA, Catalan-Soares B, Proietti F. Higher prevalence of fibromyalgia in patients infected with human T cell lymphotropic virus type I. J Rheumatol. 2006 Nov;33(11):2300–3.
12. Mori KI, Noguchi M, Matsuo M, Nomata K, Nakamura T, Kanetake H. Natural course of voiding function in patients with human T-cell lymphotrophic virus type 1-associated myelopathy. J Neurol Sci. 2004 Jan;217(1):3–6.
13. Oliveira P, De Castro NM, Carvalho EM. Urinary and sexual manifestations of patients infected by HTLV-I. Clinics. 2007 Apr;62(2):191–6.
14. Stumpf BP, Carneiro-Proietti AB, Proietti FA, Rocha FL. Higher rate of major depression among blood donor candidates infected with human T-cell lymphotropic virus type 1. Int J Psychiatry Med. 2008;38(3):345–55.
15. Darugar Q, Kim H, Gorelick RJ, Landes C. Human T-Cell Lymphotropic Virus Type 1 Nucleocapsid Protein-Induced Structural Changes in Transactivation Response DNA Hairpin Measured by Single-Molecule Fluorescence Resonance Energy Transfer. J Virol. 2008 Dec;82(24):12164–71.
16. Pettersen EF, Goddard TD, Huang CC, Couch GS, Greenblatt DM, Meng EC, et al. UCSF Chimera - A visualization system for exploratory research and analysis. J Comput Chem. 2004;25(13):1605–12.
17. Kaplan W, Littlejohn TG. Swiss-PDB Viewer (Deep View). Brief Bioinform. 2001;2(2):195–7.
18. Berman HM, Westbrook J, Feng Z, Gilliland G, Bhat TN, Weissig H, et al. The Protein Data Bank. Vol. 28, Nucleic Acids Research. 2000. p. 235–42.
19. Ramachandran S, Kota P, Ding F, Dokholyan N V. Automated minimization of steric clashes in protein structures. Proteins Struct Funct Bioinforma. 2011;79(1):261–70.
20. Dallakyan S, Olson AJ. Small-molecule library screening by docking with PyRx. Methods Mol Biol. 2015;1263:243–50.
21. O'Boyle NM, Morley C, Hutchison GR. Pybel: A Python wrapper for the OpenBabel cheminformatics toolkit. Chem Cent J. 2008;2(1).
22. Rappé AK, Casewit CJ, Colwell KS, Goddard WA, Skiff WM. UFF, a Full Periodic Table Force Field for Molecular Mechanics and Molecular Dynamics Simulations. J Am Chem Soc. 1992;114(25):10024–35.
23. Jász Á, Rák Á, Ladjánszki I, Cserey G. Optimized GPU implementation of Merck Molecular Force Field and Universal Force Field. J Mol Struct. 2019;1188:227–33.
24. Fuhrmann J, Rurainski A, Lenhof HP, Neumann D. A new Lamarckian genetic algorithm for flexible ligand-receptor docking. J Comput Chem. 2010;31(9):1911–8.
25. Morris GM, Goodsell DS, Halliday RS, Huey R, Hart WE, Belew RK, et al. Automated docking using a Lamarckian genetic algorithm and an empirical binding free energy function. J Comput Chem. 1998;19(14):1639–62.
26. Alogheli H, Olanders G, Schaal W, Brandt P, Karlén A. Docking of Macrocycles: Comparing Rigid and Flexible Docking in Glide. J Chem Inf Model. 2017;57(2):190–202.
27. Sander T, Freyss J, Von Korff M, Rufener C. DataWarrior: An open-source program for chemistry aware data visualization and analysis. J Chem Inf Model. 2015;55(2):460–73.
28. Daina A, Michielin O, Zoete V. SwissADME: A free web tool to evaluate pharmacokinetics, drug-likeness and medicinal chemistry friendliness of small molecules. Sci Rep. 2017;7.
29. Phillips JC, Braun R, Wang W, Gumbart J, Tajkhorshid E, Villa E, et al. Scalable molecular dynamics with NAMD. Vol. 26, Journal of Computational Chemistry. 2005. p. 1781–802.
30. Phillips JC, Hardy DJ, Maia JDC, Stone JE, Ribeiro J V., Bernardi RC, et al. Scalable molecular dynamics on CPU and GPU architectures with NAMD. J Chem Phys. 2020;153(4).
31. Sargsyan K, Grauffel C, Lim C. How Molecular Size Impacts RMSD Applications in Molecular Dynamics Simulations. J Chem

Theory Comput. 2017;13(4):1518–24.
32. Coutsias EA, Seok C, Dill KA. Using quaternions to calculate RMSD. J Comput Chem. 2004;25(15):1849–57.
33. Humphrey W, Dalke A, Schulten K. VMD: Visual molecular dynamics. J Mol Graph. 1996;14(1):33–8.
34. Essmann U, Perera L, Berkowitz ML, Darden T, Lee H, Pedersen LG. A smooth particle mesh Ewald method. J Chem Phys. 1995;103(19):8577–93.
35. Lam KC, Thomas ng S, hu T, Skitmore M, Cheung SO. Decision support system for contractor pre-qualification—artificial neural network model. Vol. 7, Engineering, Construction and Architectural Management. 2000. p. 251–66.
36. Xu C, Zhu J, Shang Y, Wu Q. A Distributed Conjugate Gradient Online Learning Method over Networks. Complexity. 2020;2020.
37. Teh YW, Thiery AH, Vollmer SJ. Consistency and fluctuations for stochastic gradient Langevin dynamics. J Mach Learn Res. 2016;17.
38. Evans DJ, Holian BL. The Nose-Hoover thermostat. J Chem Phys. 1985;83(8):4069–74.
39. Seeliger D, De Groot BL. Ligand docking and binding site analysis with PyMOL and Autodock/Vina. J Comput Aided Mol Des. 2010;24(5):417–22.
40. Laskowski RA, Swindells MB. LigPlot+: Multiple ligand-protein interaction diagrams for drug discovery. J Chem Inf Model. 2011;51(10):2778–86.
41. Wallace AC, Laskowski RA, Thornton JM. Ligplot: A program to generate schematic diagrams of protein-ligand interactions. Protein Eng Des Sel. 1995;8(2):127–34.
42. Lobanov MY, Bogatyreva NS, Galzitskaya O V. Radius of gyration as an indicator of protein structure compactness. Mol Biol. 2008;42(4):623–8.

5487847845**1201210**